Partial Sequencing of a Single DNA Molecule with a Scanning Tunnelling Microscope
Paper in journals : this is the first page of a paper published in ***Nature Nanotechnology*** .
[***Nature Nanotechnology***] **4**, 518-522 (2009)

LETTERS
PUBLISHED ONLINE: 5 JULY 2009 | DOI: 10.1038/NNANO.2009.155
nature nanotechnology

Partial sequencing of a single DNA molecule with a scanning tunnelling microscope

Hiroyuki Tanaka* and Tomoji Kawai*

The scanning tunnelling microscope is capable of the real-space imaging and spectroscopy of molecules on an atomic scale. Numerous attempts have been made to use the scanning tunnelling microscope to sequence single DNA molecules, but difficulties in preparing samples of long-chain DNA molecules on surfaces, and problems in reproducing results have limited these experiments[1–6]. Here, we report single-molecule DNA sequencing with a scanning tunnelling microscope by using an oblique pulse-injection method to deposit the molecules onto a copper surface. First, we show that guanine bases have a distinct electronic state that allows them to be distinguished from the other nucleic acid bases. Then, by comparing data on M13mp18, a single-stranded phage DNA, with a known base sequence[7], the 'electronic fingerprint' of guanine bases in the DNA molecule is identified. These results show that it is possible to sequence individual guanine bases in real long-chain DNA molecules with high-resolution scanning tunnelling microscope imaging and spectroscopy.

We have previously detected the characteristic electronic states of the fluorescent dye molecule fluorescein isothiocyanate (FITC) in single-molecule scanning tunnelling microscope (STM) observations and $I-V$ measurements of short strands of DNA and peptide nucleic acid (PNA) labelled with FITC[8], but we could not observe peaks in the characteristic electronic states of base molecules due to scatter and the poor signal-to-noise ratio of the $I-V$ curve[9–11]. Here, by using lock-in detection[8], we have successfully detected electronic states that are exclusively characteristic of DNA/PNA.

Figure 1 shows typical STM images of single-stranded monomers of FITC-modified PNA (FITC–TTGACC) and DNA (FITC–TTGGCC), as well as the spectroscopic data for these samples. As can be seen from the wide-area images (Fig. 1a,d), it is difficult to fully determine the base sequences of oligomers due to the existence of other adsorbed materials (thought to be nucleotide monomers, buffers and salts that were not completely eliminated in the purification process) and the diversity of the adsorbed structures of the oligomers themselves. However, by comparing two types of oligomer, it is possible to assign guanine. With FITC–TTGACC, only one base is seen to shine in the middle of the base sequence, whereas with FITC–TTGGCC there are two, as can be seen from the wide-area image (Fig. 1d) and enlarged image (Fig. 1e). Furthermore, with tunnelling spectroscopy obtained by lock-in detection, it can be seen that the guanine base molecules differ from the other base molecules and the underlying substrate in that they have a characteristic peak in the electronic state in the vicinity of an applied voltage (V_s) of −1.6 V (Fig. 1c,f). Of the four bases, it is thought that guanine is the easiest to detect because it has the lowest ionization potential[12]. To the best of our knowledge, there are no previous STM reports where the characteristic state density of base molecules, adsorbed onto a metal substrate, have been detected in this way[4,9–11,13,14].

Recent theoretical calculations[15] of DNA base molecules adsorbed on a Cu(111) surface suggest that peaks in the density of states capable of being measured by STM should exist for all four types of base molecules and not just guanine. Although the calculated energy of the first peak below the Fermi energy of the guanine/copper agrees well with our experimental values, the theoretical predictions for the other bases are inconsistent with our STM measurements. It is not understood why this characteristic electronic state occurs only for guanine bases. However, to determine if these results are also correct for real DNA, and if they are effective for sequencing, we analysed long-chain DNA strands.

The difficulties encountered in the past in sequencing single long-chain DNA molecules with the STM have been due, in part, to the unsuitability of the sample preparation methods[2]. Although researchers have managed to observe the macro structure of DNA[3,4], few studies have been able to make use of the full resolving power of the STM, that is, the clear and reproducible observation of individual nucleotides. Detailed STM imaging, spectroscopy and manipulation studies of molecules are almost always restricted to molecules that can be deposited onto a surface from the gas phase[16,17], although alternative sample preparation methods have been examined[1,18–20]. By developing a pulse-injection technique for depositing molecules onto substrates that cannot be vapour deposited (including supramolecular and biological molecules such as DNA), we have previously achieved reliable and repeatable high-resolution STM observations of the helical period of circular double-stranded (plasmid) DNA, and of the individual nucleotides in single-stranded (ss) DNA oligomers and DNA polymers[1,5,6]. However, this technique suffers from the fact that ssDNA can easily form secondary structures due to intrastrand base-pairing, with the result that sections of sufficient length to allow sequencing are rarely observed[6]. Most of the DNA stretching methods that have so far been developed for ascertaining the dynamics of DNA and analysing single-molecule genes are either performed in liquid[21] or atmospheric conditions[22], making them unsuitable for high-resolution, ultrahigh-vacuum studies. It was therefore necessary to develop a technique for stretching out ssDNA strands.

We have developed[23] a method for stretching out and fixing single-stranded M13mp18 DNA molecules (which contains 7,249 bases)[7] by using the flow effects resulting from the oblique injection[8] of a DNA solution onto a substrate using a pulse-injection technique (Fig. 2a). When the DNA solution is injected perpendicularly onto the substrate, no extended DNA is observed (see Supplementary Fig. S1). Figure 2b shows a typical wide-region STM image (400 nm wide) of an ss M13mp18 extended and fixed by oblique injection on a Cu(111) surface. Owing to the height differences at steps in the substrate, the contrast is not ideal for recognizing DNA molecules, but it is possible to recognize two DNA strands running from left to right. Figure 3 shows the image obtained over a wider area (800 nm wide). As a result of the wide scan

The Institute of Scientific and Industrial Research, Osaka University, Mihogaoka, Ibaraki, Osaka 567-0047, Japan. *e-mail: hrtanaka@sanken.osaka-u.ac.jp; kawai@sanken.osaka-u.ac.jp

▲Reprinted with permission from ***Nature Nanotechnology,*** 4, 518-522(2009). Copyright 2009 Nature Publishing Group.

The following is a comment on the published paper shown on the preceding page.

Partial Sequencing of a Single DNA Molecule with a Scanning Tunnelling Microscope

TANAKA Hiroyuki and KAWAI Tomoji
(The Institute of Scientific and Industrial Research)

Introduction

Although developments in science and technology have resulted in higher standards of living, people continue to strive for a safer society with access to personal medicine. Investigations aimed at the development of a high-speed, cheap, single-molecule-based sequencer have been performed worldwide using advanced technologies such as nanotechnology and biotechnology. Since the development of scanning tunnelling microscopy (STM), a typical technological tool that allows for the visualization and manipulation of individual molecules and atoms, researchers have attempted to sequence individual nucleotides in DNA using STM. Although several STM images showing the apparent macrostructure of DNA were reported by researchers,[1] it was concluded at about 1990 that the majority of the images represented nothing but artifacts.[2] Notwithstanding the continued efforts of researchers devoted to the STM imaging of DNA or DNA-related molecules, the general consensus seemed to suggest that it is impossible to realize high resolution STM imaging and sequencing of macromolecules such as DNA.

It became clear that one of the difficulties concerned the sample preparation method. STM achieves highest resolution under vacuum conditions. Under other conditions such as in air or liquid, the resolution of the image is easily lost by contamination. DNA molecules require pH-controlling buffer solutions, the chemical components of which (salts and buffer molecules) can lead to disturbances in high resolution STM observations. Since most of the salts and buffer can be removed by dialysis, DNA is typically deposited directly onto a surface from solution under ambient conditions and the sample is then loaded into the vacuum STM chamber. This method, however, does not provide a sufficiently clean substrate to allow for high-resolution imaging. If concentrated residual salts and buffer cover the DNA during the drying process, this can lead to additional contamination.

In an effort to overcome the aforementioned difficulties, we developed our own deposition method and became the first group to successfully achieve the high-resolution STM imaging of DNA.[3-5] In our deposition method, the DNA solution is injected directly into an ultrahigh vacuum using a pulse valve directed at a surface. Although both DNA and solvent water molecules adsorb onto the surface, the water molecules evaporate from the surface before appreciable aggregation of DNA occurs. Use of this method also minimizes the aggregation of salts and buffer onto DNA strands and therefore improves high-resolution STM imaging. It should be noted that injection of the amounts of water employed into an ultrahigh vacuum (UHV) chamber may result in a fatal crash of the expensive UHV pump system, in addition to contamination of the valuable substrate and vacuum chamber; the use of conventional UHV experiments should obviate such outcomes.

We made great strides in visualizing individual nucleotides within a DNA oligomer, in addition to imaging the macrostructure of a DNA oligomer and supramolecules. However, due to the intrastrand base-pairing within long-chain single-stranded DNAs (ssDNAs), the macromolecules are not sufficiently stretched out on the surface to facilitate efficient and reliable sequencing. Most of the DNA stretching methods that have been developed to date for ascertaining the dynamics of DNA and analyzing single-molecule genes are either performed in liquid or atmospheric conditions, making them unsuitable for high-resolution, ultrahigh-vacuum studies. It was therefore necessary that a technique be developed for stretching out ssDNA strands.

Fortunately, we recently overcame this problem by modifying our previously developed deposition method. With this new approach, the DNA solution is injected at a tilted surface.[6] This method stretches out the individual DNA molecules across the surface and allows the molecules to be imaged without removing them from the vacuum. We found that when measuring the conductance spectrum (the derivative of the current–voltage spectrum) over the four different DNA bases, guanine showed a characteristic conductance peak when the STM tip was biased at −1.6 V. This characteristic is unique to guanine. By imaging a stretched, single-stranded M13mp18 DNA molecule,[7] with the sample biased at this voltage, we obtained an image in which the guanine bases appeared larger and brighter, and therefore could readily be identified. By matching the relative position of the guanine bases with the known sequence, we were able to sequence the guanine bases and identify the imaged segment within the known sequence of a real long-chain DNA molecule.

Experimental procedure

We used two low-temperature STM systems, one (LT–STM, Omicron GmbH) and the other (USM-1200S2N1, Unisoku). Both STM chambers were cooled by liquid nitrogen, and the observation temperature was 80 K. The substrate used was a Cu(111) surface, cleaned to be atomically flat by argon ion sputtering at 773 K in ultrahigh vacuum. M13mp18 ssDNA was purchased from Bayou Biolabs and was subjected to dialysis (Slide-A-Lyzer MINI Dialysis Unit, 10,000-molecular-weight-cut-off type; Rockford) against water to remove excess buffer solution and salt. M13 mp18 DNA was dissolved in water at concentrations of 0.5 nmol l^{-1} and was deposited on clean Cu(111) surfaces using the oblique pulse injection method at room temperature(see Fig.1a).

The distance from the pulse valve to the substrate was 50 mm.

The solution was injected towards the substrate when the valve was opened for 1.5 ms. When the DNA solution was injected perpendicularly onto the substrate, no extended DNA was observed in atomic force microscopy images. When the DNA solution was injected at a slanting angle such as 45° onto the substrate, extended DNA was observed. The *dI/dV* map was measured with lock-in detection of the a.c. tunnelling current by modulating the sample bias (0.1 V r.m.s., 1 kHz) while keeping the feedback loop active.

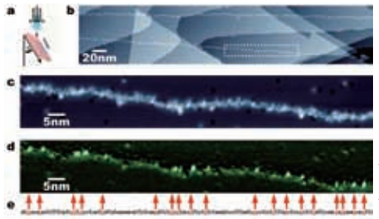

Fig. 1 Deposition and STM analysis of single-stranded M13mp18 DNA molecules on a Cu(111) surface. a, Schematic illustration of the oblique injection method. DNA strands tend to align more perpendicular than horizontal to the flow (injection) direction. The Cu(111) substrate is inclined at ~45° to the aqueous solution of DNA, which is introduced from a pulse valve. **b,** Typical wide-area image of M13mp18 (2 V, 5 pA, width 400 nm). Atomic steps in the Cu(111) substrate form a staircase surface structure. In this image, sections of M13mp18 are visualized as linear adsorbed material running from the top left to bottom right. **c,** An enlarged view of the rectangular region enclosed by the white dashed line in b (–2V, 5 pA, 100 nm). **d,** A *dI/dV* map of the same region as in **c** (–1.5 V, 20 pA, 100 nm). To maximize the detection of the density of states of guanine, the measurements were made under slightly lower bias conditions than in **c. e,** Part of the base sequence of M13mp18 obtained from a databank (the sequence of bases at positions 5322 through 5461). To facilitate comparison with the STM data, the guanine sites are indicated by red characters and are also connected by red arrows to the corresponding parts of the image.

Figure 1b shows a typical wide-region STM image (400 nm wide) of an ss M13mp18 extended and fixed by oblique injection on a Cu(111) surface. Owing to the height differences at steps in the substrate, the contrast is not ideal for recognizing DNA molecules, but it is possible to recognize two DNA strands running from left to right. Using this extended DNA, and to check whether or not it is possible to assign the individual guanine units, we measured topography images and *dI/dV* map images over the 100-nm-wide region highlighted in Fig. 1b. In the topography image of Fig. 1c, the individual nucleotides are shown as bright points, which are exceptionally bright in some places. The nucleotides that appeared brightest in the topography image also appear as clear bright points in the *dI/dV* map of Fig. 1d. For comparison, part of the known base sequence of M13mp18 is shown in Fig. 1e. The observed image and the known guanine sequence match almost perfectly, illustrating that STM can be used to sequence the guanine in real DNA.

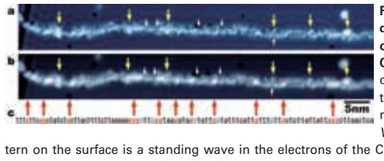

Fig.2 Bias voltage dependence on the STM imaging of M13mp18 DNA on a Cu(111) surface. a,b, Raw data obtained with the same tip on the same 70 nm × 9 nm area: Vs=0.1 V (**a**), and *Vs*=-2 V (**b**). The ripple pattern on the surface is a standing wave in the electrons of the Cu(111) surface. **c,** Part of the known base sequence of M13mp18 (the sequence of bases at positions 2911 to 3011). To facilitate comparison with the STM data, the guanine sites are indicated by red characters and are also connected by red arrows to the corresponding parts of the image. Some of the cytosine units are indicated by blue characters and the corresponding nucleotides in the STM images (**a**,**b**) are indicated by white arrows. The yellow arrows in the STM images indicate contaminants.

To make further advances towards the use of STM as a practical tool for sequencing, we must be able to recognize all four types of base molecule, and achieve greater speed and precision. In general, lock-in detection sacrifices temporal resolution for the sake of improved signal-to-noise ratio. If STM software and control mechanisms capable of finding chain-shaped polymers such as DNA can be developed, then the time taken to scan parts where the sample is not present can be greatly reduced. Savings in cost and time can also be made if sequencing is performed from the topographic image alone without using a lock-in amplifier, but it would still be necessary to use a method for identifying contamination. A method that is relatively fast and easy to implement involves comparing the STM bias dependence. That is, if guanine can be distinguished by comparing two images obtained at a value of *Vs* that is much lower than the peak in the density of states for guanine (for example, -2 V) and in fact at a value close to 0 V, then it should be possible to perform sequencing at high speed without the need for spectroscopy. As shown in Fig. 2, comparing images obtained at different bias voltages helps distinguish between DNA base molecules and contaminants: irregular points of brightness that do not vary with the bias voltage (yellow arrows in Fig. 2a) are contaminants.

The undulating pattern surrounding the DNA chain in Fig. 2a is observed at low bias conditions (*Vs* =0.1 V), and is thus a standing wave resulting from the scattering of surface electrons.[8] Compared with the image obtained with a low bias voltage, some of the nucleotides in the high bias image (*Vs*=-2 V) are brighter and thus correspond to guanine. To verify this, we compared the results with the sequence extracted from a databank (at positions 2911–3011) as shown in Fig. 2c, which can confirm if the guanine base molecules are completely matched either individually or in groups (g, gg, ggg). It can thus be seen that it is possible to recognize the guanine pattern with few errors simply by obtaining a pair of STM topographic images in this way (preferably dual bias mode). By closely examining the sections of the STM images of Fig. 2 where the nucleotides are neatly arranged, it appears as though the cytosine units are smaller than the thymine units (white arrows).

Fig.3 Example of pinpoint sequencing The false-colour STM image which measures 67 nm across, shows a DNA molecule running from bottom left to top right (the sequence of bases at positions 5084 to 5210; agaatgtccttttattactggtcgtgtgactggtgaatctgccaatgtaaataatccatttcagacgattgagcgtcaaaatgtaggtatttccatgagcgtttttcctgttgcaatggctggcgg). As can be seen, this STM image was featured on the cover of the journal. (http://www.nature.com/nnano/journal/v4/n8/covers/index.html)

Conclusions

In conclusion, by developing a method for extending and fixing DNA strands, we have taken a step towards the realization of electronic-based single-molecule DNA sequencing. Of the four bases, we were able to precisely identify guanine because the STM is able to pick up on the characteristics of its electronic state, which is largely independent of the adsorption structure. If vibrational spectroscopy is performed using inelastic electron tunnelling spectroscopy, it should be possible to identify all of the base molecules.[9] Furthermore, because STM can select a specific position of interest along a DNA strand, as shown in Fig.3, the technique could have a unique advantage in analysing, for example, single nucleotide polymorphisms.

References

[1] [1] D. Porath, *Nature Nanotech*. **4**, 476–477 (2009).
[2] C. R. Clemmer et al., *Science* **251**, 640–642 (1991).
[3] H. Tanaka et al., *J. Vac. Sci. Technol. B* **15**, 602–604 (1997).
[4] H. Tanaka et al., *Surf. Sci.* **432**, L611–L616 (1999).
[5] H. Tanaka et al., *Surf. Sci.* **539**, L531–L536 (2003).
[6] H. Tanaka et al., Japanese patent Kokoku 2005-46665 (2005).
[7] R. Ebright et al., *Gene* **114**, 81–83 (1992).
[8] M. F. Crommie et al., *Nature* **363**, 524–527 (1993).
[9] W. Ho, *J. Chem. Phys.* **117**, 11033–11061 (2002).

Zc3h12a is an RNase Essential for Controlling Immune Responses by Regulating mRNA Decay

Paper in journals : this is the first page of a paper published in ***Nature.***
[*Nature*] 458, 1185–1190 (2009)

Vol 458|30 April 2009|doi:10.1038/nature07924 nature

LETTERS

Zc3h12a is an RNase essential for controlling immune responses by regulating mRNA decay

Kazufumi Matsushita[1,3]*, Osamu Takeuchi[1,3]*, Daron M. Standley[2], Yutaro Kumagai[1,3], Tatsukata Kawagoe[1,3], Tohru Miyake[1,3], Takashi Satoh[1,3], Hiroki Kato[1,3], Tohru Tsujimura[4], Haruki Nakamura[5] & Shizuo Akira[1,3]

Toll-like receptors (TLRs) recognize microbial components, and evoke inflammation and immune responses[1–3]. TLR stimulation activates complex gene expression networks that regulate the magnitude and duration of the immune reaction. Here we identify the TLR-inducible gene *Zc3h12a* as an immune response modifier that has an essential role in preventing immune disorders. *Zc3h12a*-deficient mice suffered from severe anaemia, and most died within 12 weeks. *Zc3h12a*$^{-/-}$ mice also showed augmented serum immunoglobulin levels and autoantibody production, together with a greatly increased number of plasma cells, as well as infiltration of plasma cells to the lung. Most *Zc3h12a*$^{-/-}$ splenic T cells showed effector/memory characteristics and produced interferon-γ in response to T-cell receptor stimulation. Macrophages from *Zc3h12a*$^{-/-}$ mice showed highly increased production of interleukin (IL)-6 and IL-12p40 (also known as IL12b), but not TNF, in response to TLR ligands. Although the activation of TLR signalling pathways was normal, *Il6* messenger RNA decay was severely impaired in *Zc3h12a*$^{-/-}$ macrophages. Overexpression of Zc3h12a accelerated *Il6* mRNA degradation via its 3′-untranslated region (UTR), and destabilized RNAs with 3′-UTRs for genes including *Il6*, *Il12p40* and the calcitonin receptor gene *Calcr*. Zc3h12a contains a putative amino-terminal nuclease domain, and the expressed protein had RNase activity, consistent with a role in the decay of *Il6* mRNA. Together, these results indicate that Zc3h12a is an essential RNase that prevents immune disorders by directly controlling the stability of a set of inflammatory genes.

The innate immune responses induced by TLRs are tightly controlled, because aberrant activation of TLR responses is harmful to the host, resulting in inflammatory diseases[1–4]. TLR signalling induces the expression of several genes, although only some of these genes have been functionally characterized as immune response modifiers. Therefore, investigation of TLR-inducible genes is important for clarifying the control mechanisms of innate immune reactions. To examine TLR-induced gene expression comprehensively, we performed microarray analysis using mouse macrophages from wild-type, *Myd88*$^{-/-}$ and *Trif*$^{-/-}$ (also known as *Ticam1*$^{-/-}$) mice stimulated with lipopolysaccharide (LPS), a TLR4 ligand. We selected 214 genes in which the expression was induced more than twofold either at 1 or 4 h after stimulation in wild-type cells. Hierarchical clustering of these LPS-inducible genes showed that they could be classified into three major clusters (Supplementary Fig. 1a). Among the clusters, genes in cluster III were rapidly induced in a MyD88-dependent manner. This cluster contained, among others, *Tnf*, *Nfkbiz* and *Zfp36*. Cluster III also contained the gene encoding Zc3h12a (Supplementary Fig. 1b). Northern blot analysis confirmed that *Zc3h12a* mRNA was rapidly induced in mouse macrophages after LPS stimulation and gradually decreased with time (Supplementary Fig. 1c). Zc3h12a has a CCCH-type zinc-finger motif, and forms a family with the homologous proteins Zc3h12b, Zc3h12c and Zc3h12d. Fractionation experiments showed that the Zc3h12a protein is mainly localized in the cytoplasm, rather than in the nucleus (Supplementary Fig. 1d).

To investigate the functional roles of Zc3h12a in the control of immune responses *in vivo*, we generated *Zc3h12a*-deficient mice (Supplementary Fig. 2a and 2b). PCR with reverse transcription (RT–PCR) analysis confirmed that the expression of *Zc3h12a* was abrogated in *Zc3h12a*$^{-/-}$ macrophages (Supplementary Fig. 2c). Although *Zc3h12a*$^{-/-}$ mice are born in a Mendelian ratio, they showed growth retardation, and most of the mice spontaneously died within 12 weeks of birth (Fig. 1a). *Zc3h12a*$^{-/-}$ mice showed severe splenomegaly and lymphoadenopathy (Fig. 1b). Histological examination revealed infiltration of plasma cells in the lung, paraepithelium of the bile duct and pancreas (Fig. 1c and Supplementary Fig. 3). Plasma cells also accumulated in *Zc3h12a*$^{-/-}$ lymph nodes and spleens (Fig. 1c). In the lymph nodes, granuloma formation was observed leading to the generation of giant cells with fused macrophages. Nevertheless, inflammatory changes were not observed in either the intestine or the joints of *Zc3h12a*$^{-/-}$ mice (data not shown).

Zc3h12a$^{-/-}$ mice suffered from severe anaemia, together with an increase in white blood cells and platelets (Fig. 1d). Furthermore, *Zc3h12a*$^{-/-}$ mice developed hyperimmunoglobulinemia of all immunoglobulin isotypes tested (Fig. 1e), and plasma cells infiltrated in the lung interstitial tissues were readily stained with anti-IgG or anti-IgA antibodies (Fig. 1g). Production of anti-nuclear antibodies and anti-double-stranded-DNA antibodies were detected in *Zc3h12a*$^{-/-}$ mice (Fig. 1f). Flow cytometric analysis showed that about 70% of CD19$^+$ B cells were IgM$^-$ IgD$^-$, but immunoglobulin$^+$, indicating that most *Zc3h12a*$^{-/-}$ B cells underwent a class switch in the spleen (Fig. 2a and data not shown). Furthermore, CD138$^+$ CD19^{low} plasma cells were abundant in the spleen of *Zc3h12a*$^{-/-}$ mice (Fig. 2b). In addition, the expression of CD69 was upregulated in splenic CD3$^+$ T cells, and CD44^{high} CD62L$^-$ T cells accumulated in the periphery (Fig. 2c and Supplementary Fig. 4a). Nevertheless, the proportion of CD4$^+$ Foxp3$^+$ regulatory T cells was comparable between wild-type and *Zc3h12a*$^{-/-}$ mice (Supplementary Fig. 4b). Stimulation of splenic T cells with anti-CD3 antibody resulted in increased production of IFN-γ, but not IL-17 (Fig. 2d and Supplementary Fig. 4c). Ter119$^+$ (also known as Ly76$^+$) erythroblast population was higher in *Zc3h12a*$^{-/-}$ spleens, probably reflecting the responses to anaemia (Supplementary Fig. 4d). However, the ratios of B to T cells and of CD4$^+$ to CD8$^+$ cells were not altered in *Zc3h12a*$^{-/-}$ spleens (Supplementary Fig. 4e, f). To examine whether haematopoietic cells are sufficient for the development of disease, we transferred bone marrow cells from *Zc3h12a*$^{-/-}$ mice to recipient

[1]Laboratory of Host Defense, [2]Laboratory of Systems Immunology, WPI Immunology Frontier Research Center, [3]Research Institute for Microbial Diseases, Osaka University, 3-1 Yamada-oka, Suita, Osaka 565-0871, Japan. [4]Department of Pathology, Hyogo College of Medicine, 1-1 Mukogawa-cho, Nishinomiya, Hyogo 663-8501, Japan. [5]Research Center for Structural and Functional Proteomics, Institute for Protein Research, Osaka University, 3-2 Yamada-oka, Suita, Osaka 565-0871, Japan.
*These authors contributed equally to this work.

▲Reprinted with permission from ***Nature***, 458, 1185-1190(2009). Copyright 2009 Nature Publishing Group.